Pergamon

Tetrahedron 56 (2000) 4203–4211

TETRAHEDRON

Violene/Cyanine Hybrids as Electrochromic Systems. Part 3:[1] Heterocyclic Onium End Groups

Siegfried Hünig,[a,*] Igor F. Perepichka,[b,†] Martina Kemmer,[a] Hermann Wenner,[a] Peter Bäuerle[c,‡] and Andreas Emge[c]

[a]*Institut für Organische Chemie der Universität Würzburg, Am Hubland, D-97074 Würzburg, Germany*
[b]*L.M. Litvinenko Institute of Physical Organic & Coal Chemistry, National Academy of Sciences of Ukraine, R. Luxemburg Street 70, Donetsk 340 114, Ukraine*
[c]*Organische Chemie II, Universität Ulm, Albert-Einstein-Allee 11, D-89081 Ulm, Germany*

Dedicated to Professor Rolf Huisgen on the occasion of his 80th birthday

Received 1 March 2000; accepted 19 April 2000

Abstract—Synthesis, cyclic voltammetry (CV) and spectroelectrochemistry (SE) of tetra-onium salts $\mathbf{3}_{\mathbf{OX}}^{+\mathbf{4}}\cdot 4BF_4^-$ and $\mathbf{6}_{\mathbf{OX}}^{+\mathbf{4}}\cdot 4PF_6^-$ are presented for both systems. Cyclic voltammograms display several reduction and oxidation peaks containing at least one reversible pair. The colorless tetracations on reduction reversibly develop long wavelength absorptions. Absorption bands arise which are attributed to $\mathbf{3}_{\mathbf{RED}}^{+\mathbf{2}}$ and $\mathbf{6}_{\mathbf{RED/OX}}^{+\mathbf{2}}$, respectively. The latter is further reversibly reduced to colorless $\mathbf{6}_{\mathbf{RED}}^{\mathbf{0}}$ for which a cyclic structure with a central four-membered ring is proposed. Radical ions like **3** $(\mathbf{6})_{\mathbf{SEM}}^{\cdot+\mathbf{3}}$ and **3** $(\mathbf{6})_{\mathbf{SEM}}^{\cdot+\mathbf{1}}$ were not detected by CV or SE. PM3 calculations of $\mathbf{6}_{\mathbf{OX}}^{+\mathbf{4}}$ down to $\mathbf{6}_{\mathbf{RED}}^{\mathbf{0}}$ change and verify two perpendicular cyanine units in $\mathbf{6}_{\mathbf{RED/OX}}^{+\mathbf{2}}$ as well as the cyclic structure for $\mathbf{6}_{\mathbf{RED}}^{\mathbf{0}}$ which is of 29.86 kcal/mol more stable than the corresponding acyclic one. Systems **7**–**12** described in the literature are discussed as vinylogous examples of **A** which also display reversible two electron transfer with strong changes in color. © 2000 Elsevier Science Ltd. All rights reserved.

Introduction

Recently,[2] we have proposed a general structure **A** of violene/cyanine hybrids for electrochromic systems in which the reduced (RED) and the oxidized (OX) forms are energetically favored over the radical ions SEM (Scheme 1). By contrast, in two step redox systems of the violene type[3] SEM becomes thermodynamically stabilized and forms the colored species in common with organic electrochromics.[4] In **A**, however, both the colored and the discolored species are represented by closed shell systems from which higher persistency is to be expected.[2]

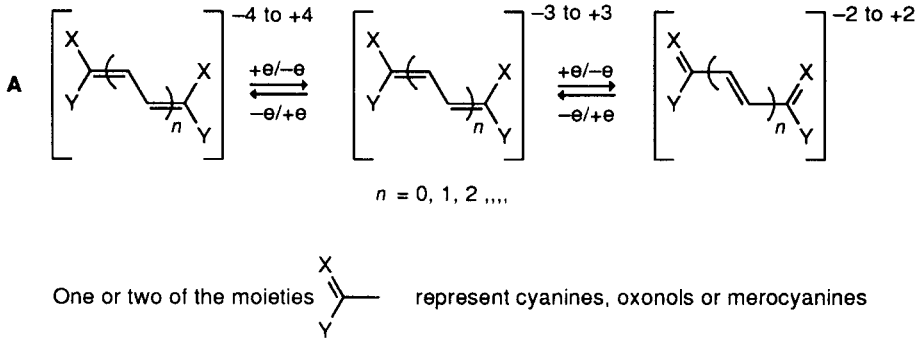

Scheme 1.

Keywords: violenes; cyanines; redox chemistry; electrochromics; heterocycles.
* Corresponding author. Tel.: +49-931-8885458; fax: +49-931-8884606; e-mail: huenig@chemie.uni-wuerzburg.de
† Fax: +380-622-558524; e-mail: i_perepichka@yahoo.com
‡ Fax: +49-731-5022840; e-mail: peter.bauerle@chemie.uni-ulm.de

0040–4020/00/$ - see front matter © 2000 Elsevier Science Ltd. All rights reserved.
PII: S0040-4020(00)00345-8

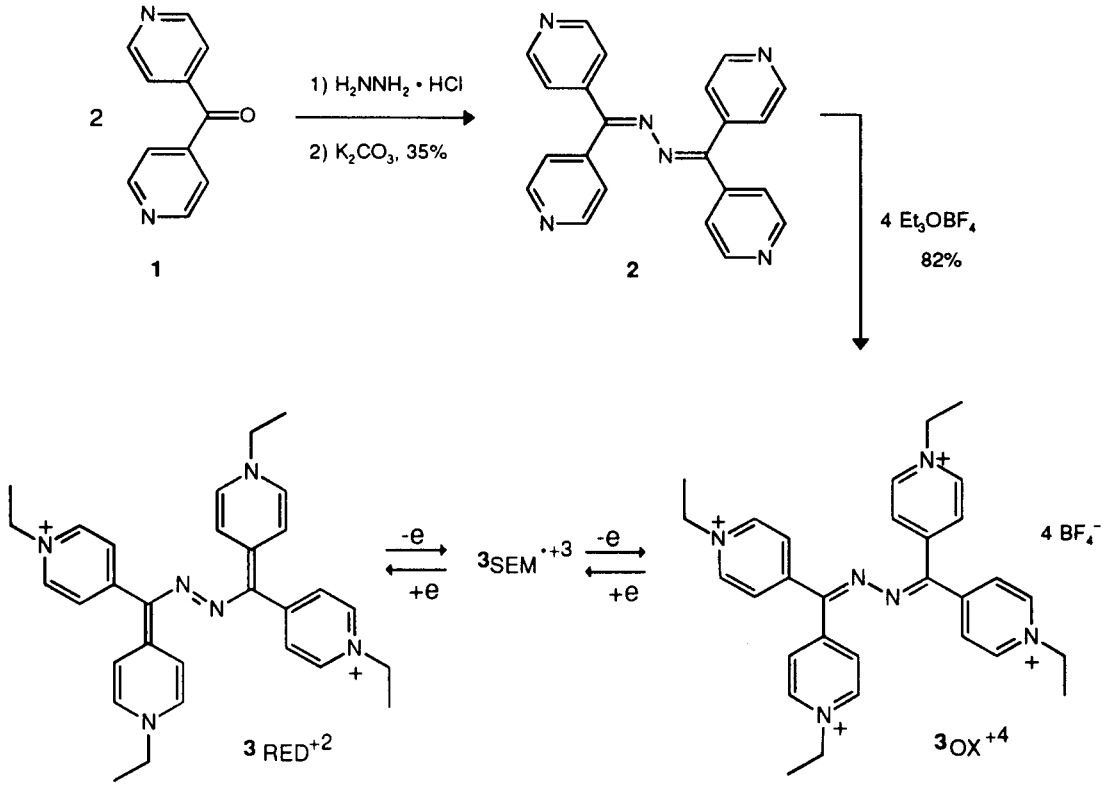

Scheme 2.

In part I,[2] the general principle **A** was exemplified by some derivatives with oxidation levels ranging from −4 to +4. Part II[1] dealt with several violene/cyanine hybrids containing for X=Y two 4-dimethylanilino groups at both ends or at one side of **A**.

We now present examples in which X and Y are verified by four heterocyclic onium ions, thereby representing the highest possible oxidation level OX^{+4} in these systems. The first two examples employing 4-pyridinium and 4-quinolinium ions as end groups have been investigated in this laboratory. The last chapter will deal with several cyanine derivatives from the literature which can be considered as members of the violene/cyanine hybrid family.

Results and Discussions

Pyridinium system 3[5]

The colorless quaternary salt $\mathbf{3}_{\mathbf{OX}}^{+4}\cdot 4BF_4^-$ is conveniently prepared according to Scheme 2.

The so far unknown azine **2** was easily obtained from 4,4′-dipyridylketone[6] (**1**) and hydrazine in yields which surely could be improved. Smooth alkylation of **2** with Meerwein's triethyloxonium tetrafluoroborate provided $\mathbf{3}_{\mathbf{OX}}^{+4}\cdot 4BF_4^-$ in good yield. As outlined in Scheme 2, $\mathbf{3}_{\mathbf{OX}}^{+4}$ on addition of two electrons is expected to turn to the colored species $\mathbf{3}_{\mathbf{RED}}^{+2}$ according to the general structure **A**

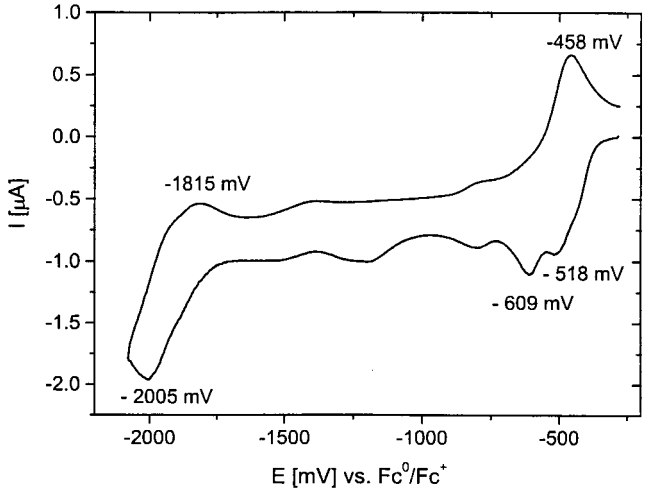

Figure 1. Cyclic voltammogram of $\mathbf{3}_{\mathbf{OX}}^{+4}\cdot 4BF_4^-$ in PhCN vs. Fc^0/Fc^+, supporting electrolyte $nBu_4N^+BF_4^-$ (0.1 M), scan rate 100 mV s^{-1}.

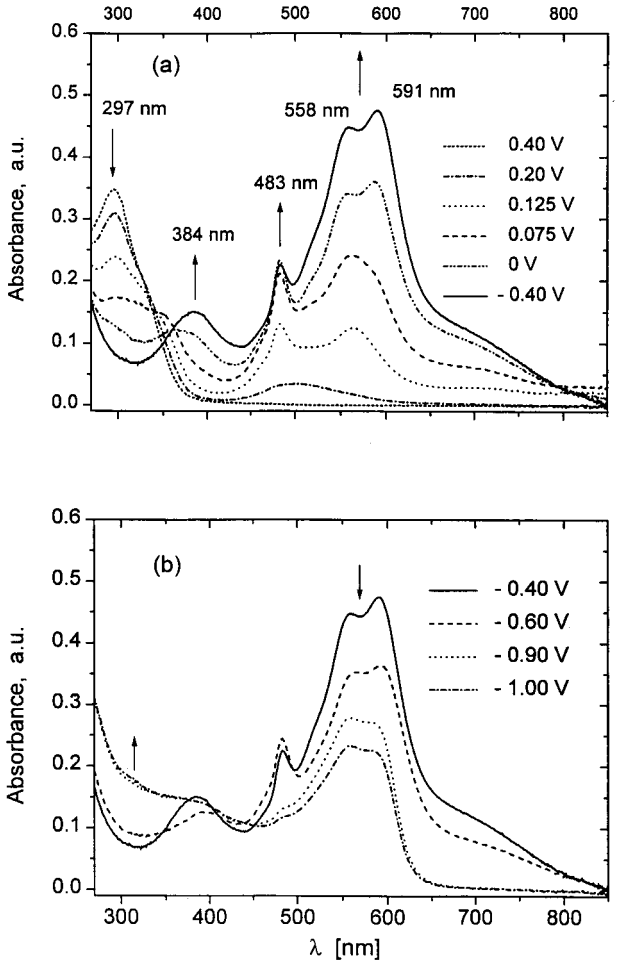

Figure 2. Spectroelectrogram of $\mathbf{3}_{OX}^{+4}\cdot 4BF_4^-$ on stepwise reduction in MeCN; supporting electrolyte $n Bu_4N^+BF_4^-$ (0.1 M); potentials are given vs. Ag/AgCl: (a) $\mathbf{3}_{OX}^{+4} \rightarrow \mathbf{3}_{RED}^{+2}$; (b) $\mathbf{3}_{OX}^{+2} \rightarrow \mathbf{3}_{RED}^{0}$.

in Scheme 1. In $\mathbf{3}_{RED}^{+2}$ an azo group is bridging two moieties of 4,4′-bispyridinemonomethine cyanine.

The cyclic voltammogram of $\mathbf{3}_{OX}^{+4}$ is not as clear cut as anticipated. On reduction two peaks arise at −518 and −609 mV (vs. Fc/Fc^+) whereas on reoxidation besides the peak at −458 mV (Fig. 1) another weak one at ca. (600 mV is to be seen only at high scan rates (500 mV s^{-1}). Repeated scans demonstrate full reversibility of the overall redox process.

One may speculate that the first reduction potential points to $\mathbf{3}_{SEM}^{\cdot+3}$ and the second one to $\mathbf{3}_{RED}^{+2}$. The radical species $\mathbf{3}_{SEM}^{\cdot+3}$, a typical violene radical,[6] is expected to exhibit a broad long but rather weak wavelength absorption which may be hidden in the SE of Fig. 2a since the isobestic point at ca. 350 nm should be sharper if only two species are equilibrating. ESR monitoring of the stepwise reduction has not yet been performed.

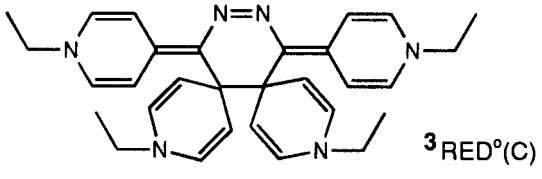

Despite these uncertainties in the CV of $\mathbf{3}_{OX}^{+4}$ the spectroelectrochemical behavior looks rather straightforward (Fig. 2). The tetracation shows no absorption between 400 and 850 nm. On stepwise reduction the solution develops a deep violet color which must be connected to the absorption maxima at 591, 558 and 483 nm. There is another weak absorption around 360–400 nm, possibly caused by the n-π^* transition of the developing azo group in $\mathbf{3}_{RED}^{+2}$. Reoxidation demonstrates the reversibility of the whole redox process. At least the bands at 558 and 591 nm have to be attributed to the two cyanine units in $\mathbf{3}_{RED}^{+2}$.

The strongly negative potential at −2.0 V with incomplete reoxidation at −1.8 V could be attributed to $\mathbf{3}_{RED}^{0}$. And, really, further stepwise cathodic shift in applied potentials on the spectroelectrogram (Fig. 2b) demonstrates disappearing of $\mathbf{3}_{RED}^{+2}$ (decreasing absorptions at 591, 558 and 483 nm). The new arising rather weak and broad absorption around 450⟶300 nm could be due to a cyclic form $\mathbf{3}_{RED}^{0(C)}$ in analogy to the tetracation derived from tetrakis 1,1,4,4-(4-dimethylaminophenyl)butadiene.[1]

Quinolinium system 6

In system **6**, four quinoline moieties are connected by their 4-positions to a C_2-unit, forming doubtlessly an overcrowded molecule. Stepwise connection of these quinoline units to a suitable C_2-precursor therefore seemed not to be advisable. However, $\mathbf{6}_{OX}^{+4}$ was easily accessible in a one-pot procedure with high yield (72%) by oxidative dimerization of the monomethine cyanine **4**.[7] This protocol adapted from Parton and Lenard[8] worked surprisingly well, although it was developed for the dimerization of trimethine- and pentamethine cyanines which hardly suffer from steric repulsion on dimerization. The cyanines are first oxidized to radical dications which dimerize (in our case to **5**). Double deprotonation (formation of two cyanine moieties) and further oxidation finally yields tetracations (here $\mathbf{6}_{OX}^{+4}$) as outlined in Scheme 3.

The cyclic voltammogram of $\mathbf{6}_{OX}^{+4}$ reveals several reduction and oxidation waves (Fig. 3). We assume that only the almost reversible redox steps characterized by their peak potentials −572/−507 mV and −1032/−982 mV (vs. Fc^0/Fc^+) are relevant for the redox process to be discussed. The whole pattern remains unchanged after several scans, indicating chemical and electrochemical overall reversibility. Although the difference in each pair of potentials, 65 and 50 mV, respectively, point to two single electron transfers, the spectroelectrograms in Fig. 4a and b point to the overall transfer of two electrons at both potentials.

However, doubtlessly strong conformational changes which will be connected with the redox process (vide infra) do not allow to compare the CV data from Fig. 3 with those of electron transfers without serious structural changes.

The pale orange solution of $\mathbf{6}_{OX}^{+4}$ in acetonitrile on stepwise reduction develops a slender absorption band at 595 nm on cost of the absorption of the starting material at 330 nm (Fig. 4a). The dark blue solution is supposed to belong to $\mathbf{6}_{RED/OX}^{+2}$ which can be considered as two directly coupled

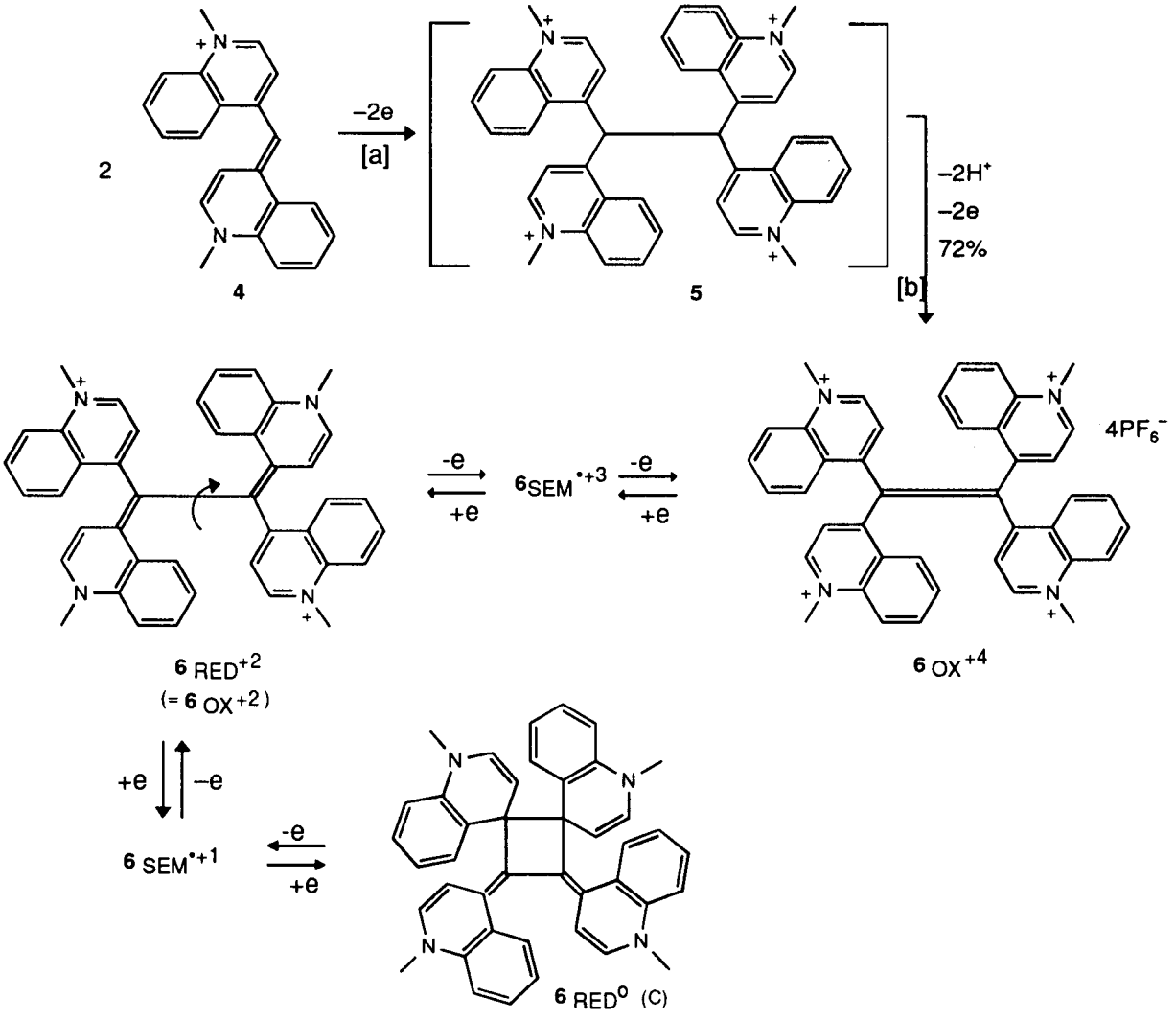

Scheme 3. Reagents: (a) $FeCl_3 \cdot 6H_2O$ in MeOH; (b) $NH_4^+PF_6^-$.

monomethine cyanines **4** (absorption of **4**, however N–Et instead of N–Me, is found at λ_{max} 590 nm[9]).

Much to our surprise, $\mathbf{6}^{+2}_{\mathbf{RED/OX}}$ after reaching its highest concentration, on further reductions gets completely (reversibly) decolorized, producing two sharp absorption maxima at 340 and 325 nm. Over the full range of reduction starting from $\mathbf{6}^{+4}_{\mathbf{OX}}$ no broad long wavelengths absorptions in

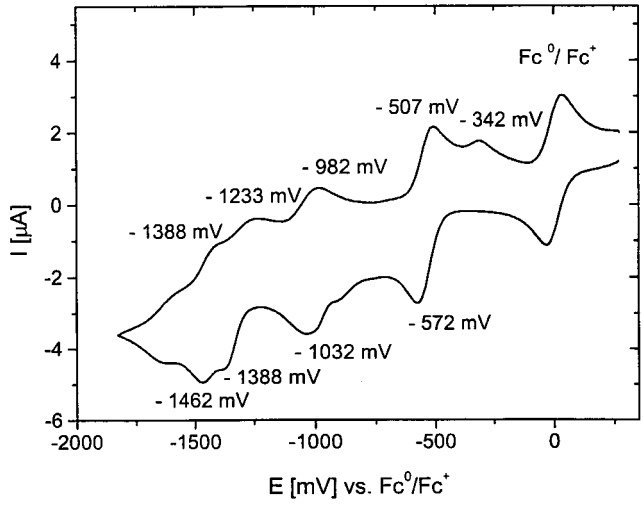

Figure 3. Cyclic voltammogram of $\mathbf{6}^{+4}_{\mathbf{OX}} \cdot 4PF_6^-$ in MeCN vs. Fc^0/Fc^-, supporting electrolyte $n Bu_4N^+PF_6^-$ (0.1 M), scan rate 100 mV s^{-1}.

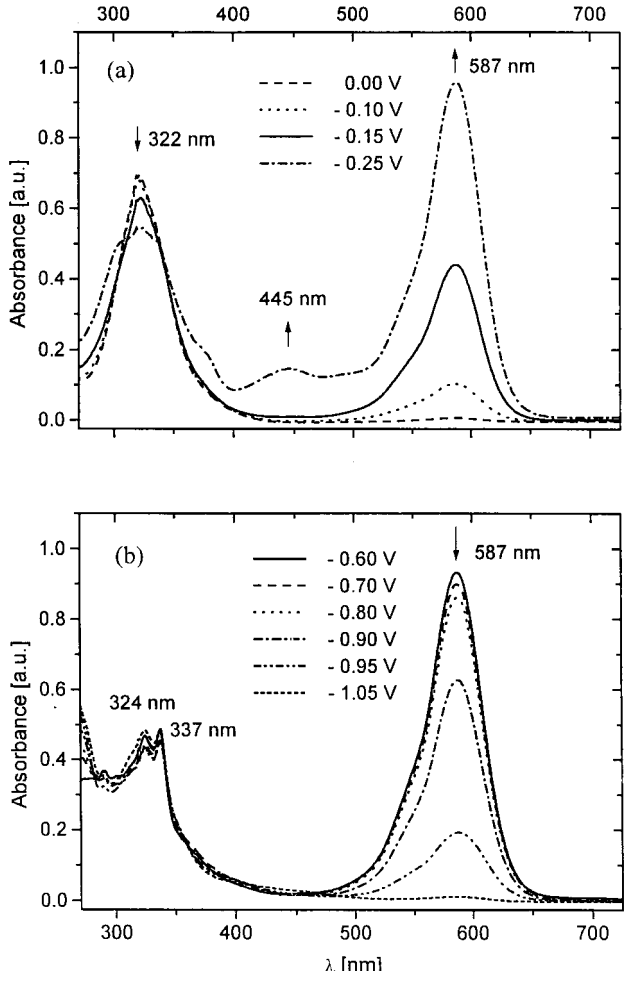

Figure 4. Spectroelectrogram of $\mathbf{6}_{OX}^{+4}\cdot 4PF_6^-$ on stepwise reduction in MeCN; supporting electrolyte nBu$_4$N$^+$PF$_6^-$ (0.1 M); potentials are given vs. Ag/AgCl: (a) $\mathbf{6}_{OX}^{+4} \rightarrow \mathbf{6}_{RED/OX}^{+2}$; (b) $\mathbf{6}_{RED/OX}^{+2} \rightarrow \mathbf{6}_{RED}^{0}$.

the near-IR region, typical for radical species of the violene type, are observed.[3] Therefore, the formation of the blue $\mathbf{6}_{RED/OX}^{+2}$ as well as its reductive decoloration, obviously to $\mathbf{6}_{RED}^{0}$, both are caused by two electron transfers. For $\mathbf{6}_{RED}^{0}$ a structure with a central cyclobutane ring is proposed as suggested by theoretical calculations (semiempirical PM3 method).

PM3 calculations of System 6

The calculated preferred conformations of the possible four oxidation levels of **6**, namely $\mathbf{6}_{OX}^{+4}$, $\mathbf{6}_{SEM}^{+3}$, $\mathbf{6}_{RED/OX}^{+2}$, $\mathbf{6}_{SEM}^{+1}$, and $\mathbf{6}_{RED}^{0}$ are pictured in Fig. 5, whereby the radical species $\mathbf{6}_{SEM}^{+3}$ and $\mathbf{6}_{SEM}^{+1}$ have not been detected in the CV of $\mathbf{6}_{OX}^{+4}$. Some relevant data are collected in Table 1 (see Scheme 4 for attribution of bond distances and torsion angles).

In $\mathbf{6}_{OX}^{+4}$ the four planar quinolinium moieties are arranged nearly perpendicular (torsion angle $\gamma \approx 82°$) to the plane of the C–C core in which the two atoms provide a typical double bond (d=135 pm). As centrosymmetric molecule the tetracation is characterized by a zero dipole moment (Table 1). This conformation is only slightly changed by addition of one electron to $\mathbf{6}_{SEM}^{+3}$: the torsion angles of the four quinolinium units (γ_A, γ_B, γ_C, γ_D) now vary between 79 and 90° and the central bond has not been affected (d=135 pm). However, in one of the end groups a pyramidalization of the nitrogen atom becomes visible indicating localization of a (partial) charge on it. This results in appearance of a substantial dipole moment in the molecule (ca. 12 D; Table 1).

A dramatic conformational change occurs in $\mathbf{6}_{RED/OX}^{+2}$ which is made responsible for the observed long wavelength absorption due to two formal cyanine units (vide supra). These two units prefer a nearly orthogonal conformation

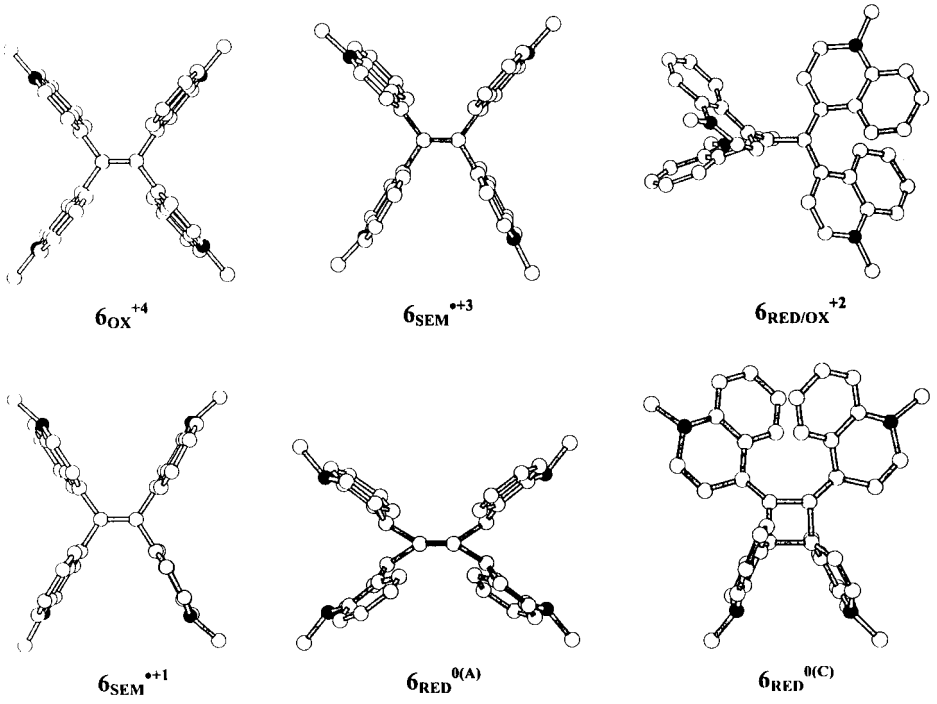

Figure 5. PM3 optimized geometries of compound **6** at various oxidation levels (hydrogen atoms are omitted; filled circles are nitrogen atoms, open circles are carbon atoms).

Table 1. Parameters of PM3-optimized structures for compound **6** at different oxidation levels (E is a heat of formation; ΔE_{A-C} is a difference in heats of formation between an acyclic structure and a cyclic structure; μ is dipole moment; attribution of a bond distances d, d_A–d_D, d_{C-D} and torsion angles α_{A-B}, α_{C-D}, γ_A–γ_D see in Scheme 4)

State	$\mathbf{6}_{OX}^{+4}$	$\mathbf{6}_{SEM}^{\cdot+3}$	$\mathbf{6}_{OX}^{+2(A)}$	$\mathbf{6}_{OX}^{+2(C)}$	$\mathbf{6}_{SEM}^{\cdot+1(A)}$	$\mathbf{6}_{SEM}^{\cdot+1(A)}$	$\mathbf{6}_{SEM}^{\cdot+1(C)}$	$\mathbf{6}_{RED}^{0(A)}$	$\mathbf{6}_{RED}^{0(A)}$	$\mathbf{6}_{RED}^{0(C)}$
E (kcal mol^{-1})	1078.33	778.44	535.45	560.54	340.58	340.60	365.56	259.73	261.89	229.87
ΔE_{A-C} (kcal mol^{-1})			−25.09		−24.96			+29.86		
HOMO (eV)	−19.56		−12.09	−12.01				−7.67	−5.22	−7.19
SOMO (eV)		−13.95 (α)[a]			−9.27 (α)	−9.26 (α)	−9.55 (α)			
		−15.25 (β)[a]			−9.50 (β)	−9.52 (β)	−9.89 (β)			
LUMO (eV)	−12.00	−9.52 (α)	−6.78	−7.40	−4.84 (α)	−4.88 (α)	−4.96 (α)	+0.17	−2.19	−0.57
		−9.82 (β)			−5.20 (β)	−5.21 (β)	−5.22 (β)			
μ (D)	0.00	12.16	3.15	18.41	13.42	13.60	14.09	0.00	0.99	0.21
d (Å)	1.349	1.354	1.480	1.349	1.364	1.356	1.356	1.298	1.507	1.466
α_{A-B} (°)	3.6	4.6	−70.0	0.3	2.7	0.2	1.5	7.2	−73.7	36.5
α_{C-D} (°)	3.6	5.2	−70.0	2.1	2.9	0.2	1.5	7.2	−73.7	12.4
d_A (Å)	1.487	1.479	1.395	1.449	1.470	1.470	1.442	1.472	1.380	1.350
d_B (Å)	1.487	1.476	1.441	1.450	1.471	1.470	1.447	1.472	1.424	1.350
d_C (Å)	1.487	1.482	1.395	1.548	1.469	1.474	1.540	1.472	1.380	1.536
d_D (Å)	1.487	1.471	1.441	1.549	1.468	1.474	1.538	1.472	1.424	1.536
γ_A (°)	−97.7	−100.8	−21.2	−94.5	−112.2	−84.6	−95.3	−74.1	−19.9	−176.0
γ_B (°)	−97.7	−98.7	−47.7	−84.4	−108.1	−89.0	−87.6	−74.1	−43.7	−173.0
γ_C (°)	−97.7	−89.5	−21.2	−115.4	−103.9	−93.1	−114.8	−74.1	−19.9	−125.3
γ_D (°)	−97.7	−95.6	−47.7	−115.5	−107.4	−85.9	−114.8	−74.1	−43.7	−125.8
d_{C-D} (Å)				1.652			1.656			1.626

[a] Orbital energies for α and β electrons.

($\alpha_{A-B}=\alpha_{C-D}=70°$) to each other thereby expanding the central C–C bond to 148 pm only. Due to the bulky quinoline groups the cyanine units cannot provide fully planar cyanine arrangements. The pairs of rings ***A***, ***C*** and ***B***, ***D*** are twisted out of plane by 21 and 48°, respectively. In accordance with the suggested cyanine character, the distances of the quinolinium rings to the central carbon atoms amount to 140 pm (rings ***A***, ***C***) and 144 pm (rings ***B***, ***D***) compared to 147–148 pm in $\mathbf{6}_{SEM}^{\cdot+3}$ and 149 pm for the four quinolinium units in $\mathbf{6}_{OX}^{+4}$. Some localization of two charges at the opposite ends is confirmed by pyramidalization of the corresponding nitrogen atoms and a diminished dipole moment (3.15 D).

On further reduction to $\mathbf{6}_{SEM}^{\cdot+1}$ the unique conformation is transformed into one which resembles $\mathbf{6}_{SEM}^{\cdot+3}$: the distance of the central C–C atoms shrinks to 136 pm and the four quinoline moieties are twisted out of plane by 85–89° (Fig. 5; Table 1: column 6). Nevertheless, this high energetic radical cation is rather flexible since a second conformation

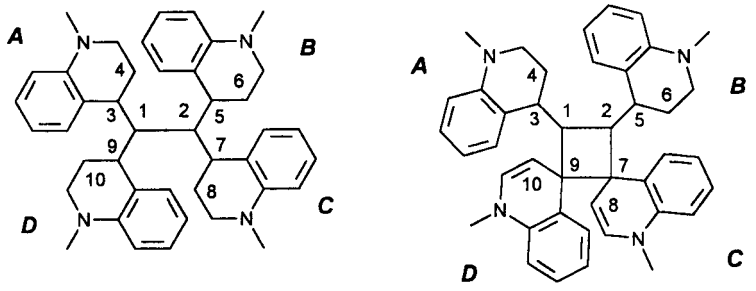

$\mathbf{6}_{OX}^{+4}$, $\mathbf{6}_{SEM}^{\cdot+3}$, $\mathbf{6}_{RED/OX}^{+2(A)}$, $\mathbf{6}_{SEM}^{\cdot+1(A)}$, $\mathbf{6}_{RED}^{0(A)}$

$\mathbf{6}_{RED/OX}^{+2(C)}$, $\mathbf{6}_{SEM}^{\cdot+1(C)}$, $\mathbf{6}_{RED}^{0(C)}$

d = C1–C2	α_{A-B} = C3–C1–C2–C5
d_A = C1–C3	α_{C-D} = C9–C1–C2–C7
d_B = C2–C5	γ_A = C4–C3–C1–C2
d_C = C2–C7	γ_B = C6–C5–C2–C1
d_D = C1–C9	γ_C = C8–C7–C2–C1
d_{C-D} = C7–C9	γ_D = C10–C9–C1–C2

Scheme 4. Attribution of bond distances and torsion angles in compound **6** (double bonds at the central C–C fragment and in the pyridine rings as well as charges and radicals on nitrogen atoms are omitted).

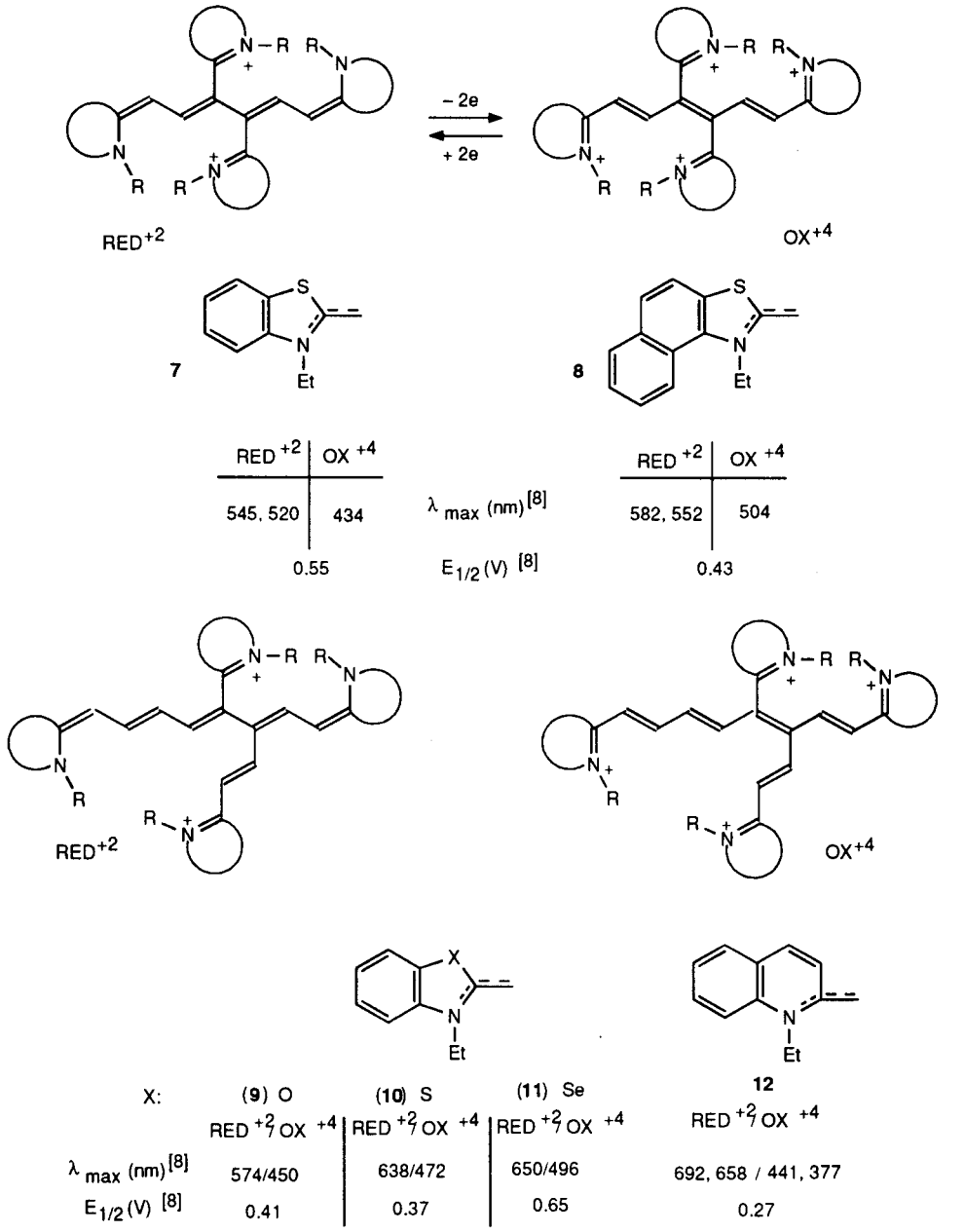

Scheme 5. Violene/cyanine hybrids derived from the general structure of Scheme 2. Examples from the literature.

of the same energy is calculated with torsion angles of 68–76° and much less planar quinoline units (cf. Table 1: column 7; the structure is not shown in Fig. 5). In both conformations of $\mathbf{6}^{+1}_{\mathbf{SEM}}$ three of four nitrogens are distinctly pyramidized, and the dipole moment is again increased.

The greatest surprise comes with the fully reduced $\mathbf{6}^{0}_{\mathbf{RED}}$. There is a highly symmetrically conformation with a very short C–C distance (130 pm) and four non-planar quinoline moieties with equal torsion angles of 74° (Fig. 5; Table 1: column 9). A second conformation (Table 1: column 10, not shown in Fig. 5) only 2.16 kcal/mol higher in energy resembles that of $\mathbf{6}^{+2}_{\mathbf{OX}}$ where the units ***A–D*** and ***B–C*** are twisted around the C–C bond (151 pm) by 74°. This conformation has pronounced biradicaloid character as follows from the decreasing HOMO–LUMO gap [cf. E_{LUMO}–$E_{\mathrm{HOMO}}$for two structures of $\mathbf{6}^{0(A)}_{\mathbf{RED}}$; column 9: 0.17 to (−7.67)=7.84 eV, column 10: −2.19 to (−5.22)= 3.03 eV]. However, both of these 'acylic' (A) conformations, $\mathbf{6}^{0(A)}_{\mathbf{RED}}$, are higher in energy compared to a 'cyclic' (C) one, $\mathbf{6}^{0(C)}_{\mathbf{RED}}$, with a four membered ring by as much as 29.86 kcal/mol which makes $\mathbf{6}^{0}_{\mathbf{RED}}$ definitely to be the preferred structure, pictured already in Scheme 3. As expected, all four uncharged nitrogen functions exist in a pyramidal geometry.

This cyclic structure is unique for $\mathbf{6}^{0}_{\mathbf{RED}}$ since calculations of such a structure as $\mathbf{6}^{+2(C)}_{\mathbf{OX}}$ and $\mathbf{6}^{+1(C)}_{\mathbf{SEM}}$ turns out to be higher in energy by ca. 25 kcal/mol in both cases, as compared with acyclic structutres, $\mathbf{6}^{+2(A)}_{\mathbf{OX}}$ and $\mathbf{6}^{+1(A)}_{\mathbf{SEM}}$, respectively.

It should be pointed out that the conformations of the

different oxidation levels of **6** shown in Fig. 5 very much resemble those calculated for violene/cyanine hybrids of the general structure **A**, where X and Y represent 4-dimethylaminophenyl groups.[1] This means that $\mathbf{6}_{\mathbf{OX}}^{+4}$ corresponds to $\mathbf{A}_{\mathbf{RED}}^{0}$ and $\mathbf{6}_{\mathbf{RED}}^{0(C)}$ to $\mathbf{A}_{\mathbf{OX}}^{+4(C)}$.

Vinylogues of A: examples from the literature[8]

Investigating the oxidation of a series of cyanines Parton and Lenard[8] found dimerization products which easily lost two protons. The new, highly colored dications behave like two cyanines connected through a single bond.

The reported completely reversible abstraction of two electrons can now be easily understood since these systems turn out to be ideal illustrations of the violene/cyanine hybrids. These dimeric cyanines are therefore presented here in such a way that their structures match the general one of Scheme 5.

In Scheme 5 examples $\mathbf{7}_{\mathbf{RED}}^{+2}$ and $\mathbf{8}_{\mathbf{RED}}^{+2}$ can be envisaged as two trimethine cyanines directly connected in two α-positions of the chain. Similarly, compounds $\mathbf{9}$–$\mathbf{12}_{\mathbf{RED}}^{+2}$ represent two pentamethine cyanines linked together in α- and γ-position. Accordingly, their intense long wavelength absorption resembles that of the corresponding cyanine dyes. On loss of two electrons, the polyenic tetracation OX^{+4} is formed. Accordingly, a strong hypsochromic shift is observed together with a depression of the molar extinction coefficients by 1/3 to 1/4. Due to the larger distances of the positive charges in $\mathbf{9}$–$\mathbf{11}_{\mathbf{RED}}^{+2}$ the oxidation potentials $E_{1/2}$ are lower by ca. 0.2 V compared to $\mathbf{7}_{\mathbf{RED}}^{+2}$ and $\mathbf{8}_{\mathbf{RED}}^{+2}$. The literature[8] does not mention any intermediate radical ions $SEM^{\cdot+3}$.

Conclusion

Both systems **3** and **6** and as vinylogues also **7**–**10** represent violene/cyanine hybrids in which the four (vinylogous) end groups X and Y are onium heterocycles connected to the central C=C double bond in their fully oxidized form $\mathbf{A}^{+4}$. They therefore are responsible for the short wavelength absorption of these electrochromic systems which turns into a long wavelengths on reversible addition of two electrons as $\mathbf{A}^{+2}$ thereby creating typical cyanine systems. Interestingly, even the full reduction of **6** to $\mathbf{6}_{\mathbf{RED}}^{0}$ occurs reversibly. The dramatic hypsochromic shift $\mathbf{6}_{\mathbf{RED/OX}}^{+2} \rightarrow \mathbf{6}_{\mathbf{RED}}^{0}$ is due to a no bond/single bond transformation with severe interruption of the conjugated systems. As anticipated radical species $\mathbf{A}_{\mathbf{SEM}}^{\cdot+3}$ and $\mathbf{A}_{\mathbf{SEM}}^{\cdot+1}$ are unimportant in all cases so that the changes in absorption are due to closed shell systems throughout.

The similarity of the conformations in the different oxidation levels from $\mathbf{6}_{\mathbf{OX}}^{+4}$ down to $\mathbf{6}_{\mathbf{RED}}^{0(C)}$ with those of the system **A** (X, Y=4-dimethylaminophenyl) from $\mathbf{A}_{\mathbf{RED}}^{0}$ to $\mathbf{A}_{\mathbf{OX}}^{+4}$ underlines the broad scope of the general violene/cyanine hybrid structure and calls for the design and investigation of further examples.

Since we are not in a position to continue our research in this field, we encourage other groups to continue.

Experimental

General

Melting points were determined on a heated microscope (Fa. Reichert) and are corrected. IR: Perkin–Elmer 1420 spectrophotometer. ^{1}H and ^{13}C NMR: Bruker AC 250 and Bruker (600 MHz) spectrometers; standardized by solvent signals.

Electrochemical measurements

Electrochemical measurements were performed with a computer-controlled EG&G PAR 273 potentiostat. The platinum working electrodes were platinum wires sealed in a glass tube with a surface of $A=0.785\ mm^2$ (∅ 1 mm) and were polished down to 0.5 μm (Bühler or Winter polishing paste) prior to use in order to get reproducible surface. The counter electrode consisted of a platinum wire, the reference electrode was a Ag/AgCl secondary electrode. Acetonitrile (Licrosolv, Merck) was filtered over aluminum oxide directly into the electrochemical cell. Benzonitrile was distilled prior to use. Tetrabutylammonium hexafluorophosphate puriss. ($Bu_4N^+PF_6^-$) or tetrafluoroborate ($Bu_4N^+BF_4^-$) were obtained from Fluka and dried in vacuo at 200°C.

General procedure for the characterization: a solution of 0.1 M $Bu_4N^+PF_6^-$ or $Bu_4N^+BF_4^-$ in PhCN or MeCN was deoxygenated with dry argon for 15 min. The corresponding compounds were characterized at a concentration of 1×10^{-3} mol l^{-1} using a scan rate of 100 mV s^{-1}.

Spectroelectrochemical measurements

UV/Vis spectra were recorded on a Perkin–Elmer Spectrophotometer Lambda 19, EG&G PAR potentiostat, model 363, was used. All optical measurements were carried out in a thin-layer electrochemical cell (distance working electrode/light conductor: 60 μm) according to Salbeck[10] incorporating a polished platinum electrode (∅ 6 mm) as the working electrode, an Ag/AgCl wire as the reference electrode and a platinum sheet as the counter electrode. Spectra were recorded in a reflection modus at the platinum electrode with the aid of a y-type optical fiber bundle. The preparation of the working electrode for optical measurements was performed in the same way as described for the preparation of working electrodes used in the electrochemical investigations.

Computational procedure

The geometries of compound **6** at all oxidation/reduction states were optimized using the MNDO-PM3 semiempirical method as implemented in the HyperChem 5.02 package of programs.[11] Polak-Ribiere algorithm was used for the optimization with SCF convergence limit of 1×10^{-5} or less; the gradient norm achieved in all the calculations was less than 0.005 kcal mol^{-1} $Å^{-1}$. Restricted Hartree–Fock (RHF) formalism was used for neutral molecules (RED), dications (OX^{+2}) and tetracations (OX^{+2}) whereas spin-unrestricted Hartree–Fock (UHF) formalism was used for radical cations ($SEM^{\cdot+1}$) and radical trications ($SEM^{\cdot+3}$). The results of

calculations are collected in Table 1 and minima energy geometries are represented in Fig. 5.

1,1,4,4-Tetrakis(4-pyridyl)-2,3-diazabuta-1,3-diene (2). 4,4′-Dipyridylketone **1** (1.00 g, 5.43 mmol) and hydrazine hydrochloride (186 mg, 2.71 mmol) in ethanol (20 mL) and chloroform (20 mL) were stirred (4 h) at 50°C and then refluxed (1 h). After addition of excess potassium carbonate the solvent was removed, the residue was dissolved in water and extracted with dichloromethane (DCM). From the organic layer an orange oil (1.8 g) was isolated which slowly crystallized. Recrystallization from acetone gave **2** (350 mg, 35%) as yellow crystals, mp 206°C. IR (KBr): $\tilde{\nu}/cm^{-1}$=1640, 1460. ^{1}H NMR (250 MHz, DMSO-d_6): 2 AA′XX′-spectra, δ=7.18 (4H), 7.28 (4H), 8.61 (4H), 8.77 (4H). ^{13}C NMR (62.9 MHz, $CDCl_3$): δ=121.9, 123.0 (2×2C, 2 py), 122.0 (2×1C), 150.3, 150.4 (2×2C, 2 py). $C_{22}H_{16}N_6$ (364.41): Calcd C 72.51, H 4.43, N 23.06; found C 72.19, H 4.48, N 22.85%.

1,1,4,4-Tetrakis(*N*-ethylpyridinium-4-yl)-2,3-diazabuta-1,3-diene tetrakis(tetrafluoroborate). ($\mathbf{3}_{\mathbf{OX}}^{+\mathbf{4}}\cdot 4BF_4^-$). To a solution of **2** (720 mg, 1.98 mmol) in dry DCM (50 mL) Et_3OBF_4 (1.44 g, 8.29 mmol) was rapidly added as a solid. A red oil was immediately formed which was isolated after stirring (12 h) by removing the solvent. Recrystallization from MeCN/Et_2O (1:2) afforded orange needles of $\mathbf{3}_{\mathbf{OX}}^{+\mathbf{4}}\cdot 4BF_4^-$ (1.35 g, 82%), mp 252°C. IR (KBr): $\tilde{\nu}/cm^{-1}$= 1640, 1460. ^{1}H NMR (600 MHz, $CDCl_3$): δ=0.66–0.70 (2d, J=7.4, 7.3 Hz, 2 ($2CH_3$), 2.35, 2.44 (2t, J=7.4, 7.3 Hz, 2 ($2CH_2$); 2 AA′XX′-spectra: 5.77, 5.85 (2×2H), 6.44, 6.65 (2×2H). ^{13}C NMR (62.9 MHz, CD_3CN): δ=7.71, 17.88, 18.67, 18.72 (4×CH_3), 59.82 (2 CH_2), 60.12 (2 CH_2), 129.27 (4 py-C_3), 130.77 (2 py-C_3), 147.18 (2 py-C_4), 147.66 (2 py-C_4), 150.51 (4 py-C_2), 158.39 (4 py-C2). $C_{30}H_{36}N_6B_4F_{16}$ (828.24): Calc C 43.51, H 4.38, N 10.15; found C 42.01,[12] H 4.31, N 9.93%.

Tetrakis(*N*-methylquinolinium-4-yl)ethene tetrakis(hexafluorophosphate). ($\mathbf{6}_{\mathbf{OX}}^{+\mathbf{4}}\cdot 4PF_6^-$). By adaption of Ref. 8 iron (III) chloride hexahydrate (1.08 g, 4.0 mmol) in water (20 mL) was slowly added to a solution 1,1′-dimethyl-4,4′-quinocyanine hexafluorophosphate $\mathbf{4}^+\cdot PF_6^-$ (889 mg, 2.00 mmol) in methanol (400 mL). After stirring (30 min) some precipitate was removed and ammonium hexafluorophosphate (4.1 g, 25 mmol) in water (300 mL) was added. Thereby the red solution turned colorless. On evaporation of the methanol (rotavapor) colorless crystals were formed. The crude product was recrystallized from MeCN/ethyl acetate yielding $\mathbf{6}_{\mathbf{OX}}^{+\mathbf{4}}\cdot 4PF_6^-$ (850 mg, 72%), mp 245°C. IR (KBr): $\tilde{\nu}/cm^{-1}$=3520 s, 3090 vs, 1695 vs, 1590 s, 1610, 1620 s, 1530 vs, 1370 s, 1320 s, 1260 s, 1100 s, 900–800 vs. ^{1}H NMR (250 MHz, $CDCl_3$): δ=2.12 (d, 12H, 4CH_3), 4.57 (4H, H-2), 4.69 (4H, H-3), 7.49–9.24 (m, 16H, H-5,6,7,8). ^{13}C NMR (62.9 MHz, CD_3CN): δ=46.6 (CH_2), 47.7 (CH_2), 120, 4 (C=C), 124.3 (C-2), 127.5 (C-3), 128.4 (C-4), 133.1 (C-8), 137.3 (C-7), 141.0 (C-5), 149.2 (C-6). $C_{42}H_{36}N_4P_4F_{24}$ (1181.0): Calcd C 42.21, H 3.41, N 4.76; found C 40.21,[12] H 3.27, N 4.68 %.

Acknowledgements

Financial support by the Volkswagen-Stiftung, BASF AG/ Ludwigshafen (BMFT project 03 M 4067 6) and Fonds der Chemischen Industrie is highly acknowledged. I. F. P. thanks the Alexander von Humboldt-Stiftung for a post-doctoral fellowship (1995–1997) to conduct some of his research work in Würzburg.

References

1. Part II: Hünig, S.; Kemmer, M.; Wenner, H.; Barbosa, F.; Gescheidt, G.; Perepichka, I. F.; Bäuerle, P.; Emge, A.; Peters, K. *Chem. Eur. J.* **2000**, in press.
2. Part I: Hünig, S.; Kemmer, M.; Wenner, H.; Perepichka, I. F.; Bäuerle, P.; Emge, A.; Gescheid, G. *Chem. Eur. J.* **1999**, *5*, 1969–1973.
3. Hünig, S. *Chimia* **1978**, *32*, 91–93.
4. (a) Shelepin, I. V.; Ushakov, O. A.; Karpova, N. I.; Barachevskii, V. A. *Elektrokhimiya* **1977**, *13*, 32–37; (b) Shelepin, I. V.; Gavrilov, V. I.; Barachevskii, V. A.; Karpova, N. I. *Elektrokhimiya* **1977**, *13*, 404–405; (c) Ushakov, O. A.; Shelepin, I. V.; Barachevskii, V. A.; Katyshev, E. G. *Elektrokhimiya* **1978**, *14*, 319–322; (d) Byker, H. J. In *Electrochromic Materials II;* Ho, K.-C., McArthur, D. A., Eds.; PV 94-2, 3–13.
5. Already briefly discussed in Ref. 2.
6. Minn, F. I.; Trichilo, Ch.I.; Hurt, Ch.I.; Filipescu, N. *J. Am. Chem. Soc.* **1970**, *92*, 3600–3610.
7. Prepared according to Berlin, I.; Riester, O. *Houben Weyl;* Thieme: Stuttgart, 1972; Vol. 1d, pp 252–253. Alkylation was performed with dimethylsulfate and the cyanine precipitated as its PF_6 salt, mp 225°C.
8. Parton, R. L.; Lenard, J. R. *J. Org. Chem.* **1990**, *55*, 49–57.
9. Bloch, D.; Hamer, F. M. *Phot J.* **1928**, *68*, 21.
10. Salbeck *J. Electroanal. Chem.* **1992**, *340*, 169–195.
11. HyperChem, Release 5.02 for Windows95/NT, 1997. Molecular Modelling System, Hypercube Inc., Gainesville, Florida, USA.
12. In accordance with earlier experiences in heterocyclic BF_4 and PF_6 salts 1–2% less carbon is found than calculated. We assume a systematic error in the intensity of the V.p.c. signals in the combustion machine.